Liquid Crystals
Publication details, including instructions for authors and subscription information:
http://www.tandfonline.com/loi/tlct20

Chiral discotic derivatives of 1,3,5-triphenyl-6-oxoverdazyl radical

Aleksandra Jankowiak[a], Damian Pociecha[b], Jacek Szczytko[c] & Piotr Kaszyński[ad]
[a] Organic Materials Research Group, Department of Chemistry, Vanderbilt University, Nashville, TN, USA
[b] Department of Chemistry, University of Warsaw, Warsaw, Poland
[c] Institute of Experimental Physics, Faculty of Physics, University of Warsaw, Warsaw, Poland
[d] Faculty of Chemistry, University of Łódź, Łódź, Poland
Published online: 21 Aug 2014.

Liquid Crystals, 2014
Vol. 41, No. 11, 1653–1660, http://dx.doi.org/10.1080/02678292.2014.947345

Chiral discotic derivatives of 1,3,5-triphenyl-6-oxoverdazyl radical

Aleksandra Jankowiak[a], Damian Pociecha[b], Jacek Szczytko[c] and Piotr Kaszyński[a,d]*

[a]*Organic Materials Research Group, Department of Chemistry, Vanderbilt University, Nashville, TN, USA;* [b]*Department of Chemistry, University of Warsaw, Warsaw, Poland;* [c]*Institute of Experimental Physics, Faculty of Physics, University of Warsaw, Warsaw, Poland;* [d]*Faculty of Chemistry, University of Łódź, Łódź, Poland*

(*Received 13 May 2014; accepted 18 July 2014*)

Two derivatives of 1,3,5-aryl-6-oxoverdazyl containing two 3,4,5-trioctyloxyphenyl and one 3,4,5-tri((*S*)-3,7-dimethyloctyloxy)phenyl group in position C(3) (**1b**) or N(1) (**1c**) were investigated by thermal, X-ray diffraction and magnetic methods. The results were compared to those obtained for achiral derivative **1a** containing three 3,4,5-trioctyloxyphenyl groups. All three compounds exhibit an ordered columnar hexagonal phase, $Col_{h(o)}$, and for chiral derivatives, **1b** and **1c**, a superstructure with doubled periodicity was found. The introduction of the three chiral alkoxy substituents in **1a** lowered the mesophase stability by about 50 K and induced a Col_h phase in **1c**. Thermochromic analysis showed a hypsochromic shift upon formation of the $Col_{h(o)}$ phase similar for all three derivatives **1** (~0.3 eV), which coincides with a 5% drop in effective magnetic moment, μ_{eff}, for **1c**. Analysis of magnetisation data in a range of 2–370 K at 200 Oe revealed weak antiferromagnetic interactions ($\theta = -4$ K) in the $Col_{h(o)}$ phase.

Keywords: discotic; verdazyl radical; chiral; thermochromism; magnetic analysis; powder XRD; synthesis

1. Introduction

Among the many characteristics of discotic liquid crystals sought for practical applications,[1–3] semiconduction and ability to generate photocurrents [4–6] are the most desired. The efficiency of the charge transport in such soft materials depends, among others, on the organisation of molecules, defects and proximity (overlap) of the π-systems.[7] Conformational and steric requirements of substituents in molecules forming discotic phases typically prevent close contact of the π-systems. In some achiral systems, e.g. triphenylenes [8] and hexabenzocoronenes,[7,9] the close molecular packing in columnar ordered and plastic phases results from a spontaneous helical twist in the columns (spontaneous symmetry breaking).[10] Overall, for non-chiral molecules, helical columns with opposite handiness are formed in equal amounts giving rise to a racemic bulk material. For materials that already have twisted columns formed by achiral molecules, a uniform sense of handiness of the helical twist is achieved by using peripheral alkyl chains containing stereogenic centres.[7] The same substitution in some other discogens transforms the columnar hexagonal (Col_h) to a columnar rectangular (Col_r) phase.[11]

Recently, we demonstrated that substituted triphenyl derivatives of verdazyl, a π-delocalised radical, form discotic hexagonal phases.[12–14] We have investigated three series of compounds containing 3,4,5-trialkoxyphenyl [12] (such as **1a**), 3,4,5-trialkylsulfanylphenyl [13] and a mixture of both substituents.[14] The results demonstrated that the alkylsulfanyl derivatives form a disordered columnar hexagonal 3D phase ($Col_{h(3D)}$) below 60°C, presumably with a helical structure. In contrast, the alkoxy derivatives, including the octyloxy derivative **1a**, form a broad-range ordered columnar hexagonal phase ($Col_{h(o)}$), with a correlation length along the columns of at least 370 Å at 30°C and pronounced thermochromism upon the formation of the mesophase. In both series of compounds, photocurrent was detected, and the hole mobility μ_h was found to be in the order 10^{-3} cm^2 V^{-1} s^{-1} in the mesophase. The tighter molecular packing in the ordered phase is also evident from magnetisation studies, which demonstrated a 4% decrease of the effective magnetic moment, μ_{eff}, at the $I \rightarrow Col_{h(o)}$ transition. Further improvement of the π–π overlap and hence increase of the photocurrent and spin–spin interactions in this type of compounds could be achieved by using stereogenic centres in the side chains.

Here, we report two derivatives **1b** and **1c** carrying three alkyl chains with stereogenic centres, the (*S*)-3,7-dimethyloctyl ($C_{10}H_{21}$*), and analyse their effect on the supramolecular structure and phase stability. We probe the phase structure by the X-ray diffraction (XRD) method and investigate its impact on molecular packing through thermochromic and magnetic methods.

*Corresponding author. Email: piotr.kaszynski@vanderbilt.edu

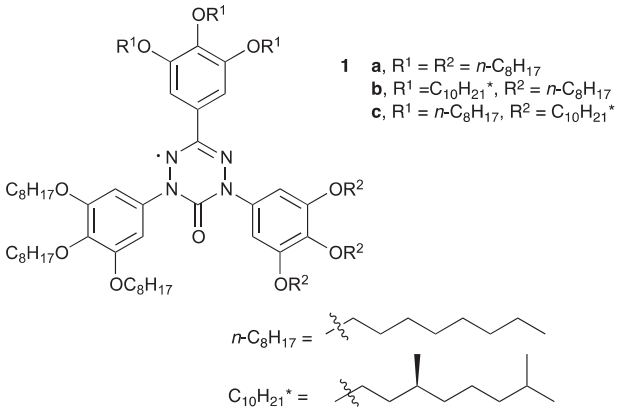

2. Results

2.1. Synthesis

Chiral derivatives **1b** and **1c** were obtained following the Milcent method [15] that was previously [12] used for the preparation of **1a** (Scheme 1). Thus, a reaction of appropriate hydrazine **2** and benzaldehyde **3** gave crude hydrazone **4**, which upon treatment with triphosgene yielded carbonyl chloride **5**. After isolation and purification, the chloride **5** was reacted with hydrazine **2** in benzene. The resulting tetrazine **6** was partially purified and oxidised with PbO_2 to give radical **1** in ~10% overall yield. The requisite chiral aldehyde **3*** was obtained from bromide **7*** [11] by lithiation followed by a reaction with dimethylformamide (DMF), according to a similar procedure [16] (Scheme 2). Lithiation of **7*** with *t*-BuLi and reaction with di-*tert*-butyl azodicarboxylate (DTBAD) gave the protected hydrazine **8***, which was deprotected with trifluoromethanesulfonic acid (TfOH) to give the crude hydrazine **2***, according to a general procedure.[17] The bromide **7*** was obtained by alkylation of 5-bromopyrogallol with tosylate **9***, which, in turn, was obtained from (*S*)-3,7-dimethyloctanol (ee >98%).

2.2. Thermal analysis

Analysis of compounds in series **1** by thermal differential scanning calorimetry (DSC) and polarized optical microscopy (POM) methods demonstrated that both red, waxy chiral derivatives, **1b** and **1c**, exhibit liquid crystalline behaviour at ambient temperature and above (Table 1), with clearing temperatures lower than that for the achiral derivative **1a** by about 50 K. In contrast to **1a** and **1b**, chiral compound **1c** exhibits two mesophases as shown in Figure 1. The higher temperature, narrow-range phase has a small enthalpy of *Col–Iso* transition (6.5 kJ mol^{-1}) and relatively small thermal hysteresis of about 3 K. In contrast, the *Col–Col* phase transition has an enthalpy nearly four times greater than

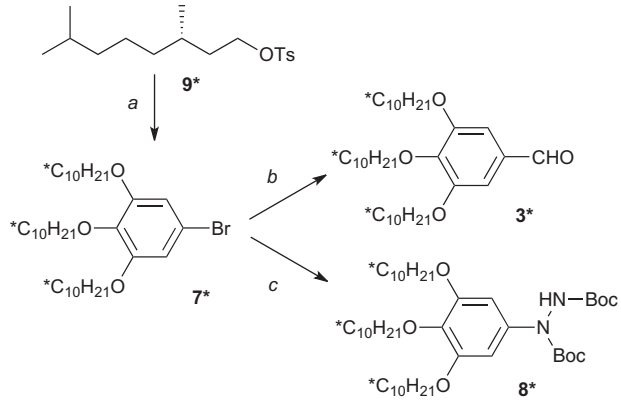

Scheme 2. Synthesis of chiral intermediates. Reagents and conditions: (a) 5-bromopyrogallol, K_2CO_3, acetone, Aliquat, 78%; (b) *n*-BuLi, DMF, H_3O^+, 70%; (c) *t*-BuLi, *t*-BuOCON = NCOOBu-*t* (DTBAD), 60%.

Table 1. Transition temperatures (°C) and enthalpies (kJ mol^{-1}, in italics) for **1**.[a]

1	R^1 R^2	
a[b]	C_8H_{17} C_8H_{17}	$Col_{h(o)}$ 127 (*55.5*) I[b]
b	$*C_{10}H_{21}$ C_8H_{17}	$Col_{h(o)}$ 73 (*34.6*) I
c	C_8H_{17} $*C_{10}H_{21}$	$Col_{h(o)}$ 67 (*25.2*) Col_h 78 (*6.5*) I

Notes: [a]Determined by DSC (5 K min^{-1}) in the heating mode: Cr = crystalline; Col_h = columnar hexagonal; $Col_{h(o)}$ = columnar hexagonal ordered; I = isotropic. [b]Ref.[12].

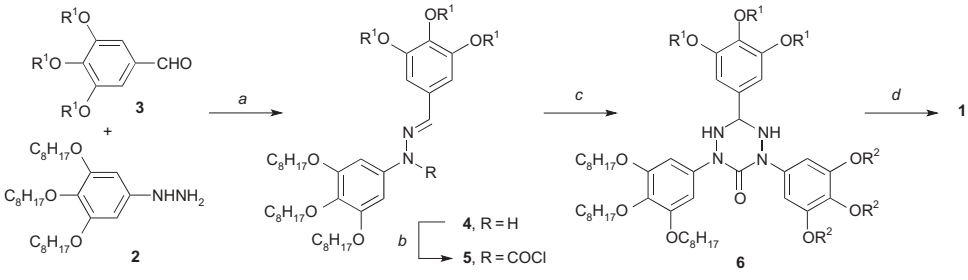

Scheme 1. Synthesis of 6-oxoverdazyls **1**. Reagents and conditions: (a) EtOH, cat. AcOH, reflux; (b) $CO(OCCl_3)_2$, pyridine, CH_2Cl_2, rt, room temperature; (c) **2**, Et_3N, benzene, 50°C; (d) PbO_2, Na_2CO_3, Toluene/MeCN.

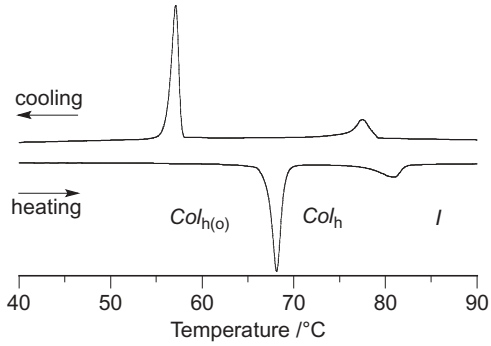

Figure 1. DSC trace of **1c**. The heating and cooling rates are 5 K min^{-1}.

that of the *Col–Iso* transition and a significantly larger hysteresis (11 K, Figure 1).

Optical textures obtained on cooling of an uncovered thick sample of **1c** or **1b** between glass plates are typical for a columnar mesophase (Figure 2). Textures observed for two phases of **1c** are essentially identical (Figure 2a and 2b). Similarly, little change in the texture is observed at the *Col–Col* phase transition for **1c** in a 5 μm planar cell (Figure 2c).

2.3. *Electronic absorption spectra and thermochromism*

Further information about the supramolecular structures of the mesophase was obtained for **1b** and **1c** by UV-vis spectra recorded for thin-film samples at ambient temperature.

Solution spectra of all three derivatives **1** are identical, resulting from the same chromophore. They exhibit low-intensity absorption bands in the visible range, with maxima at about 610 nm and 500 nm and a moderate-intensity absorption band at about 210 nm, characteristic for the 3,4,5-trialkoxyphenyl group (Figure 3).

Visible spectra recorded for thin films of **1** in the isotropic phase and mesophase demonstrated a substantial thermochromic effect upon the formation of the ordered hexagonal phase in all three samples. Results shown in Table 2 demonstrate that for **1a** the formation of a *Col* mesophase is associated with a

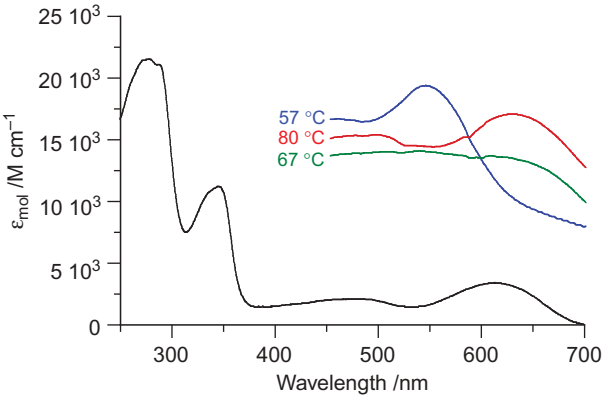

Figure 3. (colour online) Electronic absorption spectra for **1b** in hexane (black) and for a thin film of **1c** on cooling (inset: isotropic phase (80°C, red), $Col_h \rightarrow Col_{h(o)}$ phase transition (67°C, green) and $Col_{h(o)}$ (57°C, blue), arbitrary units).

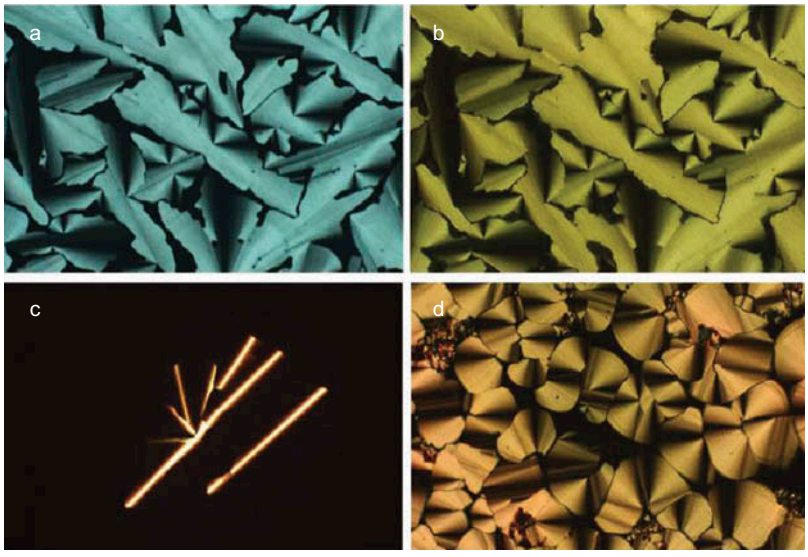

Figure 2. (colour online) Optical textures of (a) Col_h phase in **1c** at 77°C, (b) $Col_{h(o)}$ of **1c** phase at 55°C, (c) $Col_{h(o)}$ of **1c** in a planar 5 mm cell at 58°C and (d) $Col_{h(o)}$ of **1b** phase at 50°C.

Table 2. Lowest energy absorption maxima **1** of the isotropic (*Iso*) and columnar ($Col_{h(o)}$) phases.[a]

1	R^1 R^2	λ_{max}/nm *Iso*	λ_{max}/nm $Col_{h(o)}$	$\Delta\lambda_{max}$ (ΔE)/nm (meV)
a	C_8H_{17} C_8H_{17}	627	542	–85 (+310)
b	$*C_{10}H_{21}$ C_8H_{17}	625	541	–84 (+308)
c	C_8H_{17} $*C_{10}H_{21}$	627	634[b]	+7 (–22)
		627	543.5	–83.5 (+304)

Notes: [a]Recorded in the transmission mode. [b]Col_h phase.

hypsochromic shift of 310 meV, which is largest in the series and also larger than that previously observed for the decyloxy analogue (282 meV).[12] A replacement of three octyloxy groups in **1a** with three $*C_{10}H_{21}O$ substituents at the C(3) position has relatively little effect on the shift, while placing chiral chains at the N(1) position results in slightly smaller hypsochromic shift by several meV. This trend is consistent with decreasing π–π overlap caused by increasing steric demands of the liquid-like larger alkyl chains.

A plot of the low-energy absorption band maximum as a function of temperature (Figure 4) provides further details of the thermochromic effect in **1c**. At low temperature in the hexagonal ordered phase ($Col_{h(o)}$), the λ_{max} value is about 543 nm. Upon heating, the position of the maximum slightly shifts to 542 nm and at the phase transition to the columnar disordered phase, in a range of 2 K shifts to 634 nm. In the middle of the $Col_h \rightarrow Col_{h(o)}$ phase transition range, at 67°C the spectrum represents an approximate superimposition of spectra obtained for both ordered and disordered phases (Figure 3). Further heating leads to a decrease of the λ_{max} value to 627 nm in the isotropic phase. This small bathochromic shift between the *Iso* and Col_h phases is typical for other discotic verdazyls.[14] Upon cooling of the sample from *Iso* to $Col_{h(o)}$ phase, λ_{max} changes in the opposite direction with about 5 K hysteresis (Figure 4).

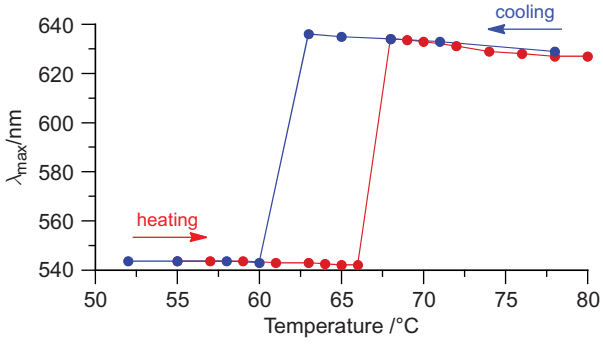

Figure 4. (colour online) Low-energy absorption maximum λ_{max} of **1c** as a function of temperature on heating (red) and cooling (blue).

2.4. *X-ray diffraction*

XRD analysis confirmed the existence of two columnar hexagonal phases in derivative **1c** by revealing the six-fold symmetry of the structure clearly visible in the pattern obtained for an aligned sample (for details see Supplemental data). The upper temperature phase can be identified as a disordered type, Col_h, since its diffractogram contains only one diffused signal in the high-angle range, reflecting liquid-like ordering of molecules along columns and a sharp Bragg reflection in the low-angle range (Figure 5). The lattice parameter (column diameter) is comparable to the molecular size (Table 3). The XRD pattern of the lower temperature phase is much richer and exhibits a number of sharp signals that can be indexed to a 2D hexagonal lattice with the lattice parameter doubled with respect to the Col_h phase (Table 3). Fitting of the XRD pattern demonstrates that all except one sharp reflections are due to the 2D hexagonal structure of columns (for details see Supplemental data); the only remaining signal at 3.9 Å can be attributed to molecular core correlation along the column stack.[12] Fitting procedure revealed also the presence of a broad signal in the high-angle region reflecting molten state of aliphatic tails. It should be

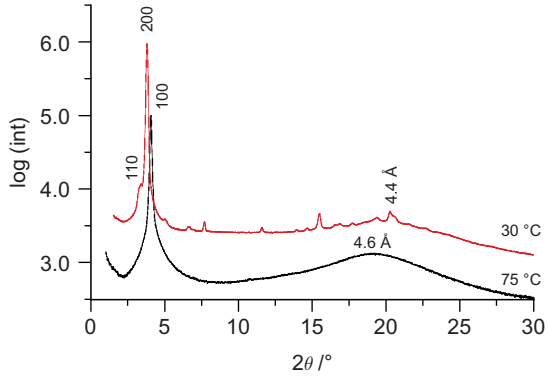

Figure 5. (colour online) XRD pattern for **1c** at 75°C (black) and 30°C (red) with partial indexing for Col_h and $Col_{h(o)}$ phases obtained on cooling from the isotropic phase.

Table 3. Lattice parameters for **1.**

1	Temp/°C	Lattice parameters (Å)	Phase
a[a]	115	a = 26.35	$Col_{h(o)}$
b	74	a = 53.18	$Col_{h(o)}$
	25	a = 52.74	$Col_{h(o)}$
c	75	a = 25.33	Col_h
	57	a = 25.53	Col_h
	55	a = 53.12	$Col_{h(o)}$
	25	a = 52.95	$Col_{h(o)}$

Note: [a]Ref. [12].

stressed, however, that the main electron density modulations are still related to the presence of columns having single molecule in the cross-section; diffraction signals related to superstructure with doubled periodicity are much weaker than signals originating from the fundamental structure. The reflection related to intermolecular distance along the column axis is sharp in the lower temperature phase, which points to an ordered type phase, $Col_{h(o)}$.[1]

In derivative **1b**, XRD methods revealed only one mesophase (for details see Supplemental data), which was identified as an ordered columnar hexagonal phase, $Col_{h(o)}$, similar to the lower temperature phase of **1c**. Also, the doubling of the columnar structure with respect to molecular diameter is observed. The observed XRD patterns do not permit assignment nor exclude the presence of a helical structure in the columns in both derivatives.

Hexagonal phases with a superlattice are rare. One example of such a phase was observed for the decyloxy analogue of **1a**,[12] in which doubling of the unit diameter was manifested by the appearance of sub-harmonic of the main (100) signal of the hexagonal lattice. In the present case, the modulation of the electron density in **1b** and **1c** is different, and the sub-harmonic of the main signal of the hexagonal lattice is absent; instead sub-harmonic of the (110) signal is clearly visible (for details see Supplemental data).

2.5. *Magnetisation measurements*

Magnetic studies at 200 Oe revealed paramagnetic behaviour of **1c** in the liquid crystalline and isotropic phases, with increasing antiferromagnetic interactions upon phase transition and lowering temperature (Figure 6).

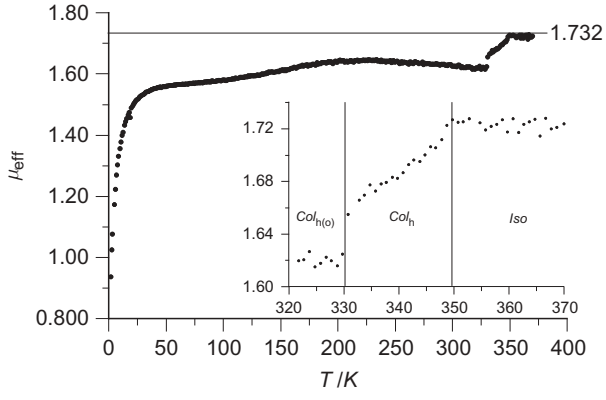

Figure 6. Effective magnetic moment, μ_{eff}, for **1c** versus temperature measured on cooling at 200 Oe (1 K min^{-1}). The horizontal line marks μ_{eff} = 1.732. The inset shows high-temperature data and the vertical lines mark phase transitions.

Assuming ideal paramagnetic behaviour in the isotropic phase, diamagnetic and impurity correction was established using the Curie–Weiss law with θ = –4 K (for details see Supplemental data). The effective magnetic moment (μ_{eff}) in the isotropic phase (>353 K) is close to the value of 1.732 for an ideal paramagnet and corresponds to 99 ± 0.5% of spins (Figure 6). Upon phase transition to the Col_h phase at 359 K, the μ_{eff} value continuously decreases to about 1.63 at 330 K at the phase transition to $Col_{h(o)}$ phase. These changes in μ_{eff} exhibit hysteresis (for details see Supplemental data) consistent with that observed in thermal analysis in Figure 1.

Cooling of the sample below 300 K in the $Col_{h(o)}$ phase results in a small, but reproducible maximum at about 225 K, followed by a rapid decrease below 50 K due to increasing antiferromagnetic interactions. The average value of μ_{eff} in the $Col_{h(o)}$ in a temperature range of 150–320 K was found to be 1.63 ± 0.01, which corresponds to 94 ± 0.5% of paramagnetic spins. These results are similar to those found [12] for **1a** and indicate that spins remain largely isolated at >150 K.

3. Summary and conclusions

Experimental data demonstrate that substitution of three chiral groups $C_{10}H_{21}$* for C_8H_{17} groups in **1a** results in significant destabilisation of the columnar $Col_{h(o)}$ phase and induction of a disordered Col_h phase. The $Col_{h(o)}$ phase in the two chiral derivatives exhibits superstructure with a doubled cell constant, which is absent in **1a**. The Col_h–$Col_{h(o)}$ and *Iso*–$Col_{h(o)}$ phase transitions are accompanied by strong thermochromism and a small change of effective magnetic moment μ_{eff}. The two regioisomers, *C*-chiral (**1b**) and *N*-chiral (**1c**), differ in their thermal properties: the $Col_{h(o)}$ phase is more destabilised for *N*-chiral (**1c**) than for *C*-chiral (**1b**) isomer. Overall thermochromism and magnetisation data indicate comparable intracolumn intermolecular interactions for all the three derivatives **1** in the $Col_{h(o)}$ phase, which appear stronger than those in the decyloxy analogue of **1a**. Thus, impact of chiral alkyl chains on molecular packing in the $Col_{h(o)}$ phase of **1a** is minimal.

4. Experimental part

4.1. *General*

Reagents and solvents were obtained commercially. Reactions were carried out under Ar, and subsequent manipulations were conducted in air. Nuclear Magnetic Resonance (NMR) spectra were obtained at 128 MHz (^{11}B) and 400 MHz (^{1}H) in $CDCl_3$. ^{1}H NMR spectra

were referenced to the solvent. Details and additional results of XRD and magnetisation measurements are provided in the Electron Spray Ionisation (ESI). Optical microscopy and phase identification were performed using a polarised microscope equipped with a hot stage. Thermal analysis was obtained using a TA Instruments DSC using small samples of about 0.5–1.0 mg.

4.2. Electronic absorption spectra

UV-vis spectra for **1b** were recorded in spectroscopic grade hexane at a concentration of 5–35 × 10^{-6} M. Extinction coefficients were obtained by fitting the maximum absorbance at 211 nm against concentration in agreement with Beer's law.

Visible spectra for neat **1** that was placed between two glass slides were obtained on cooling at temperatures about 10 K above and then 10 K below the *Col–Iso* phase transition for each compound using a hot stage mounted in a UV spectrometer. For **1c**, the spectrum of Col_h phase was recorded in the middle of the phase range.

4.3. Powder XRD measurements

X-ray diffraction experiments in broad-angle range were performed with Bruker D8 GADDS (Cu Kα radiation, Göbel mirror, point collimator, Vantec 2000 area detector) equipped with a modified Linkam heating stage. For small-angle diffraction experiments, Bruker Nanostar system was used (Cu Kα radiation, cross-coupled Göbel mirrors, three pinhole collimation, Vantec 2000 area detector). Samples were prepared in the form of a thin film or a droplet on heated surface. The X-ray beam was incident nearly parallel to sample surface.

4.4. General procedure for 6-oxoverdazyls 1

To a solution of carbamoyl chloride **5b** or **5c** [12] (0.5 mmol) in dry benzene (15 mL), a solution of freshly prepared 3,4,5-trioctyloxyphenylhydrazine [17] (**2**) or 3,4,5-tris((*S*)-3,7-dimethyloctyloxy)phenylhydrazine (**2***, 0.6 mmol) and Et_3N (0.65 mmol) in dry benzene (5 mL) was added. The mixture was stirred for 2 h at 50°C. A 1% solution of HCl was added, organic products were extracted (CH_2Cl_2), extracts dried (Na_2SO_4) and solvents evaporated. The residue was passed through a short silica gel column (hexane/CH_2Cl_2, 2:1) to give a fraction containing tetrazine **6** identified by characteristic signals in the ^{1}H NMR: δ 4.71 (*d, J* = 8.5 Hz, 2H) and 5.46 (*t, J* = 8.5 Hz, 1H) (**6c**: high-resolution mass spectrometry (HRMS), calcd for $C_{98}H_{174}N_4O_{10}$ $[MH]^+$: *m/z* 1567.3224; found *m/z* 1567.3271).

A mixture of partially purified tetrazine **6** (0.1 mmol), anhydrous Na_2CO_3 (106 mg, 1.0 mmol) and PbO_2 (478 mg, 2.0 mmol) in a mixture of toluene (6 mL) and MeCN (1.5 mL) was stirred overnight at room temperature. The dark reaction mixture was passed through a silica gel plug (CH_2Cl_2), and the crude product was further purified on a silica gel column (hexane/CH_2Cl_2, 6:1) to give radical **1** as a red waxy solid in overall yields of about 10% based on **5**. The solid was recrystallised several times from AcOEt at –78°C.

4.4.1. 1,5-bis-(3,4,5-trioctyloxyphenyl)-3-(3,4,5-tris((*S*)-3,7-dimethyloctyloxy)phenyl)-6-oxoverdazyl (**1b**)

UV (hexane) λ_{max} (log ε) 613 (3.53), 479 (3.32), 346 (4.05), 288 (4.32), 278 (4.33), 211 (4.92). Anal. calcd for $C_{98}H_{171}N_4O_{10}$: C, 75.19; H, 11.01; N, 3.58. Found: C, 75.06; H, 11.05; N, 3.51.

4.4.2. 1,3-Bis-(3,4,5-trioctyloxyphenyl)-5-(3,4,5-tris((*S*)-3,7-dimethyloctyloxy)phenyl)-6-oxoverdazyl (**1c**)

Anal. calcd for $C_{98}H_{171}N_4O_{10}$: C, 75.19; H, 11.01; N, 3.58. Found: C, 75.44; H, 11.02; N, 3.58.

4.5. 3,4,5-Tris((*S*)-3,7-dimethyloctyloxy)phenylhydrazine (2*)

Following a general procedure,[17] to a solution of TfOH (5 mmol) in CF_3CH_2OH (1 mL), a solution of 1,2-bis(*tert*-butoxycarbonyl)-1-(3,4,5-tris((*S*)-3,7-dimethyloctyloxy)phenylhydrazine (**8***, 1 mmol) in CH_2Cl_2 (1 mL) was added under Ar at –40°C. The mixture was stirred for 2 min, washed with saturated $NaHCO_3$, organic products were extracted (CH_2Cl_2), extracts dried (Na_2SO_4) and solvents evaporated to give crude deprotected hydrazine **2***, which was used quickly for further steps without purification: ^{1}H NMR (400 MHz, $CDCl_3$) δ 0.86 (*d, J* = 6.6 Hz, 18H), 0.91 (*d, J* = 6.7 Hz, 3H), 0.93 (*d, J* = 6.6 Hz, 6H), 1.11–1.20 (*m*, 8H), 1.21–1.37 (*m*, 10H), 1.44–1.61 (*m*, 6H), 1.63–1.75 (*m*, 3H), 1.76–1.88 (*m*, 3H), 3.92–4.05 (*m*, 6H), 6.07 (*s*, 2H).

4.6. 3,4,5-Tris((*S*)-3,7-dimethyloctyloxy)benzaldehyde (3*)

3,4,5-Tri-(*S*)-3,7-dimethyloctyloxybenzaldehyde was obtained in 70% yield from 1-bromo-3,4,5-tris((*S*)-3,7-dimethyloctyloxy)benzene (*7**) by lithiation with *n*-BuLi and subsequent treatment with DMF according to a general procedure [16] for preparation of aldehydes: $[\alpha]^{25}_D$ = – 4.01 (hexane, *c* = 1.4); ^{1}H NMR (400 MHz, $CDCl_3$) δ 0.86 (*t, J* = 6.6 Hz,

6H), 0.87 (*t, J* = 6.6 Hz, 12H), 0.92 (*t, J* = 6.6 Hz, 3H), 0.95 (*t, J* = 6.5 Hz, 6H), 1.11–1.22 (*m*, 8H), 1.23–1.38 (*m*, 10H), 1.47–1.58 (*m*, 6H), 1.60–1.78 (*m*, 3H), 1.79–1.93 (*m*, 3H), 4.02–4.14 (*m*, 6H), 7.09 (*s*, 2H), 9.84 (*s*, 1H); HRMS, calcd for $C_{37}H_{67}O_4$ $[MH]^+$: *m/z* 575.5034; found: *m/z* 575.5046.

4.7. 3,4,5-Tris((S)-3,7-dimethyloctyloxy) benzaldehyde 3,4,5-trioctyloxyphenylhydrazone (4b)

To a solution of crude 3,4,5-trioctyloxyphenylhydrazine [17] (1.3 mmol) and benzaldehyde **3*** (450 mg, 0.8 mmol) in a mixture of EtOH (2 mL) and tetrahydrofuran (THF) (2 mL), 1 drop of AcOH was added. The mixture was refluxed for 1 h under Ar, cooled, solvent was evaporated and traces of AcOH were removed on vacuum to give 800 mg (~90% yield) of crude hydrazone **4b** (~70% pure by ^{1}H NMR), which was used for the next step without additional purification: ^{1}H NMR (400 MHz, $CDCl_3$) characteristic signals: δ 6.33 (*s*, 2H), 6.85 (*s*, 2H), 7.4 (br *s*, 1H), 7.56 (*s*, 1H).

4.8. 3,4,5-Tris((S)-(3,7-dimethyloctyloxy) benzaldehyde α-chloroformyl-3,4,5-trioctyloxyphenylhydrazone (5b)

To a solution of crude hydrazone **4b** (1.20 g, 1.3 mmol) in dry CH_2Cl_2 (5 mL), pyridine (0.13 mL, 1.6 mmol) followed by triphosgene (386 mg, 1.3 mmol) were added under Ar. The mixture was stirred at ambient temperature for 4 h, 1% HCl was added, organic products were extracted (CH_2Cl_2), extracts were dried (Na_2SO_4) and solvent was evaporated. The crude product was purified on a short silica gel column (hexane/CH_2Cl_2, 3:1) to give 550 mg (50% yield) of chloride **5b** as a yellowish viscous oil: ^{1}H NMR (400 MHz, $CDCl_3$) δ 0.86 (*d, J* = 6.7 Hz, 12H), 0.85–0.90 (*m*, 6H), 0.88 (*t, J* = 6.3 Hz, 9H), 0.91 (*d, J* = 6.6 Hz, 3H), 0.93 (*d, J* = 6.5 Hz, 6H), 1.10–1.20 (*m*, 8H), 1.22–1.39 (*m*, 36H), 1.40–1.92 (*m*, 22H), 3.93 (*t, J* = 6.5 Hz, 4H), 3.96–4.12 (*m*, 8H), 6.40 (*s*, 2H), 6.85 (*s*, 2H), 7.23 (*s*, 1H); HRMS, calcd for $C_{68}H_{120}ClN_2O_7$ $[MH]^+$: *m/z* 1111.8779; found: *m/z* 1111.8785.

4.9. 1-Bromo-3,4,5-tri((S)-3,7-dimethyloctyloxy) benzene (7)*

A mixture of 5-bromopyrogallol (1.30 g, 6.4 mmol), K_2CO_3 (5.2 g, 38.0 mmol) and (*S*)-3,7-dimethyloctyl *p*-toluenesulfonate **(9***, 6.00 g, 19.2 mmol**)** with cat. amounts of Aliquat in dry DMF (10 mL) was stirred for 18 h at 60°C. The resulting precipitation was filtered, water was added, organic products were extracted (hexanes), extracts were dried (Na_2SO_4) and solvent was evaporated. The crude product was purified on a short silica gel column (hexane/CH_2Cl_2, 8:1) to give 3.12 g (78% yield) of bromide **7*** as a colourless oil: $[\alpha]^{25}_D$ = –4.1 (hexane, *c* = 2.4); ^{1}H NMR (400 MHz, $CDCl_3$) δ 0.86 (*d, J* = 6.6 Hz, 6H), 0.87 (*d, J* = 6.6 Hz, 12H), 0.91 (*d, J* = 6.7 Hz, 3H), 0.93 (*d, J* = 6.6 Hz, 6H), 1.10–1.22 (*m*, 8H), 1.23–1.38 (*m*, 10H), 1.47–1.58 (*m*, 6H), 1.60–1.78 (*m*, 3H), 1.79–1.93 (*m*, 3H), 3.90–4.02 (*m*, 6H), 6.68 (*s*, 2H); HRMS, calcd for $C_{36}H_{66}BrO_3$ $[MH]^+$: *m/z* 625.4198; found *m/z* 625.4190. Anal. calcd for $C_{36}H_{65}BrO_3$: C, 69.09; H, 10.47. Found: C, 69.34; H, 10.63.

4.10. 1,2-Bis(tert-butoxycarbonyl)-1-(3,4,5-tris ((S)-3,7-dimethyloctyloxy)phenyl)hydrazine (8)*

To a solution of bromobenzene **7*** (1.50 g, 2.4 mmol) in dry THF (20 mL), *t*-BuLi (1.7 M in pentane, 5.3 mmol) was added under Ar at −78°C. The mixture was stirred at this temperature for 1.5 h, and a THF (5 mL) solution of DTBAD (610 mg, 2.6 mmol) was added dropwise. The mixture was stirred at −78°C for 0.5 h, then 1 h at room temperature and then quenched with 5% HCl. The organic products were extracted (Et_2O), extracts were dried (Na_2SO_4), solvents were evaporated and the residue was passed through a silica gel plug (hexane/CH_2Cl_2 then CH_2Cl_2) to give 0.90 g (60% yield) of protected hydrazine **8*** as a viscous oil: $[\alpha]^{25}_D$ = –2.9 (hexane, c = 2.2); ^{1}H NMR (400 MHz, $CDCl_3$) δ 0.87 (*d, J* = 6.6 Hz, 18H), 0.90 (*d, J* = 5.8 Hz, 3H), 0.93 (*d, J* = 6.3 Hz, 6H), 1.11–1.20 (*m*, 8H), 1.23–1.37 (*m*, 10H), 1.51 (*s*, 18H), 1.47–1.58 (*m*, 6H), 1.62–1.75 (*m*, 3H), 1.76–1.88 (*m*, 3H), 3.90–4.02 (*m*, 6H), 6.66 (*s*, 2H), 6.70 (brs, 1H); HRMS, calcd for $C_{46}H_{85}N_2O_7$ $[MH]^+$: *m/z* 777.6351; found: *m/z* 777.6364.

4.11. (S)-3,7-Dimethyloctyl p-toluenesulfonate (9)*

Toluenesulfonyl chloride (3.60 g, 19.0 mmol) was added to a solution of (*S*)-3,7-dimethyloctan-1-ol (3.00 g, 19.0 mmol) and pyridine (1.61 mL, 20.0 mmol) in CH_2Cl_2 (10 mL) at 0°C. The mixture was kept at this temperature for 5 h, then at room temperature overnight. Hexane was added (20 mL), and the resulting precipitation was filtered. The solvents were evaporated, and the residue was passed through a silica gel plug (hexane/CH_2Cl_2, 4:1) to give 5.0 g (84% yield) of pure tosylate **9*** as a colourless oil: $[\alpha]^{25}_D$ = –2.0 (benzene, *c* = 1.4) [lit.[18] (*R*) isomer: $[\alpha]_D$ = +2.0 (benzene, *c* = 4.0)]; ^{1}H NMR (400 MHz, $CDCl_3$) δ 0.80 (*d, J* = 6.5 Hz, 3H), 0.85 (*d, J* = 6.6 Hz, 6H), 0.99–1.31 (*m*, 6H), 1.37–1.54 (*m*, 3H), 1.61–1.71 (*m*, 1H), 2.45 (*s*, 3H), 4.01–4.11 (*m*, 2H), 7.34 (*d, J* = 6.6 Hz, 2H), 7.79 (*d, J* = 6.6 Hz, 2H); HRMS, calcd for $C_{17}H_{28}NaO_3S$ $[MNa]^+$: *m/z* 335.1651; found: *m/z* 335.1664. Anal.

calcd for $C_{17}H_{28}O_3S$: C, 65.35; H, 9.03. Found: C, 65.86; H, 9.07.

4.12. (S)-3,7-Dimethyloctan-1-ol

(*S*)-(–)-β-citronellol (5.00 g, 32.1 mmol, purchased from Aldrich; $[\alpha]^{25}_D$ = –4.07 (EtOH, c = 1.4), $[\alpha]^{25}_D$ = –5.27 (neat), lit.[19] $[\alpha]^{24}_D$ = –3.65 (EtOH, c = 1.0), lit.[20] $[\alpha]^{20}_D$ = –5.18 (neat) 98% ee) was catalytically reduced at 50 psi in EtOH (50 mL), in the presence of 10% Pd/C (1.0 g). Crude alcohol was purified by short-path distillation (90°C/0.5 mmHg, lit.[21] 52°C/0.1 mmHg): $[\alpha]^{25}_D$ = –5.06 (MeOH, *c* = 4.4), $[\alpha]^{25}_D$ = –3.93 ($CHCl_3$, *c* = 4.0), $[\alpha]^{25}_D$ = –5.01 (neat) [lit.[21] $[\alpha]^{25}_D$ = –4.77 (neat)].

Funding

This work was supported by NSF grant [CHE-1214104]. We are grateful to Prof. Andrzej Twardowski for funding the SQUID measurements. We thank Ms Ola Kruczkowska for her assistance with preparation of this manuscript.

Note

1. This phase could also be considered as soft crystalline; however, a broad signal observed in the high-angle region that could be attributed to the molten alkyl chains points to the liquid crystalline, although ordered, nature of this columnar phase.

Supplemental data

Supplemental data for this article can be accessed here.

References

[1] Boden N, Movaghar B. Applicable properties of columnar discotic liquid crystals. In: Demus D, Goodby J, Gray GW, Spiess H-W, Vill V, editors. Handbook of liquid crystals. Vol. 2B. New York: Wiley-VCH; 1998. p. 781–798.
[2] Bushby RJ, Kawata K. Liquid crystals that affected the world: discotic liquid crystals. Liq Cryst. 2011;38:1415–1426.
[3] Kaafarani BR. Discotic liquid crystals for opto-electronic applications. Chem Mater. 2011;23:378–396. doi:10.1021/cm102117c
[4] Bushby RJ, Lozman OR. Photoconducting liquid crystals. Curr Opin Solid State Mater Sci. 2002;6:569–578. doi:10.1016/S1359-0286(03)00007-X
[5] Kumar S. Discotic liquid crystals for solar cells. Curr Sci. 2002;82:256–257.
[6] Li Q, Li L. Photoconducting discotic liquid crystals. In: Ramamoorthy A, editor. Thermotropic liquid crystals: recent advances. Dordrecht: Springer; 2007. p. 297–322.
[7] Pisula W, Kastler M, Wasserfallen D, Mondeshki M, Piris J, Schnell I, Müllen K. Relation between supramolecular order and charge carrier mobility of branched alkyl hexa-peri-hexabenzocoronenes. Chem Mater. 2006;18:3634–3640. doi:10.1021/cm0602343
[8] Fontes E, Heiney PA, De Jeu WH. Liquid-crystalline and helical order in a discotic mesophase. Phys Rev Lett. 1988;61:1202–1205. doi:10.1103/PhysRevLett.61.1202
[9] Wu J, Watson MD, Zhang L, Wang Z, Müllen K. Hexakis(4-iodophenyl)-peri-hexabenzocoronene-A versatile building block for highly ordered discotic liquid crystalline materials. J Am Chem Soc. 2004;126:177–186. doi:10.1021/ja037519q
[10] Vera F, Serrano JL, Sierra T. Twists in mesomorphic columnar supramolecular assemblies. Chem Soc Rev. 2009;38:781–796. doi:10.1039/b800408k
[11] Lee H, Kim D, Lee H-K, Qiu W, Oh N-K, Zin W-C, Kim K. Discotic liquid crystalline materials for potential nonlinear optical applications: synthesis and liquid crystalline behavior of 1,3,5-triphenyl-2,4,6-triazine derivatives containing achiral and chiral alkyl chains at the periphery. Tetrahedron Lett. 2004;45:1019–1022. doi:10.1016/j.tetlet.2003.11.085
[12] Jankowiak A, Pociecha D, Monobe H, Szczytko J, Kaszyński P. Thermochromic discotic 6-oxoverdazyls. Chem Commun. 2012;48:7064–7066. doi:10.1039/c2cc33051b
[13] Jankowiak A, Pociecha D, Szczytko J, Monobe H, Kaszyński P. Photoconductive liquid-crystalline derivatives of 6-oxoverdazyl. J Am Chem Soc. 2012;134:2465–2468. doi:10.1021/ja209467h
[14] Jankowiak A, Pociecha D, Szczytko J, Monobe H, Kaszyński P. Liquid crystalline radicals: discotic behavior of unsymmetrical derivatives of 1,3,5-triphenyl- 6-oxoverdazyl. J Mater Chem C. 2014;2:319–324. doi:10.1039/c3tc31984a
[15] Milcent R, Barbier G, Capelle S, Catteau J-P. New general synthesis of tetrahydro-1,2,4,5-tetrazin-3 (2H)-one derivatives and stable 3,4-dihydro-3-oxo-1,2,4,5-tetrazin-1(2H)-yl radical derivatives. J Heterocycl Chem. 1994;31:319–324. doi:10.1002/jhet.5570310210
[16] Jankowiak A, Debska Ż, Romański J, Kaszyński P. Synthesis of 3,4-dialkylsulfanyl- and 3,4,5-trialkylsulfanyl derivatives of bromobenzene and benzaldehyde. J Sulfur Chem. 2012;33:1–7. doi:10.1080/17415993.2011.644554
[17] Jankowiak A, Kaszyński P. Synthesis of oleophilic electron-rich phenylhydrazines. Beils J Org Chem. 2012;8:275–282. doi:10.3762/bjoc.8.29
[18] Schmid M, Barner R. Totalsynthese von natürlichem α-tocopherol. 2. mitteilung. Aufbau der seitenkette aus (−)-(S)-3-methyl-γ-butyrolacton. Helv Chim Acta. 1979;62:464–473. doi:10.1002/hlca.19790620211
[19] Belani JD, Rychnovsky SD. A concise synthesis of ent-cholesterol. J Org Chem. 2008;73:2768–2773. doi:10.1021/jo702694g
[20] Dalisay DS, Quach T, Molinski TF. Liposomal circular dichroism. assignment of remote stereocenters in plakinic acids K and L from a plakortis−xestospongia sponge association. Org Lett. 2010;12:1524–1527. doi:10.1021/ol100249v
[21] Jha SK, Cheon K-S, Green MM, Selinger JV. Chiral optical properties of a helical polymer synthesized from nearly racemic chiral monomers highly diluted with achiral monomers. J Am Chem Soc. 1999;121:1665–1673. doi:10.1021/ja983202s